

# Quaternary structure and functional properties of *Penaeus monodon* hemocyanin

Mariano Beltramini<sup>1</sup>, Nadia Colangelo<sup>1</sup>, Folco Giomi<sup>1</sup>, Luigi Bubacco<sup>1</sup>, Paolo Di Muro<sup>1</sup>, Nadja Hellmann<sup>2</sup>, Elmar Jaenicke<sup>2</sup> and Heinz Decker<sup>2</sup>

<sup>1</sup> Department of Biology, University of Padova, Padova, Italy

<sup>2</sup> Institute of Molecular Biophysics, Mainz, Germany

## Keywords

allosteric interactions; hemocyanin; oxygen binding; *Penaeus monodon*; quaternary structure

## Correspondence

M. Beltramini, Department of Biology,  
University of Padova, Viale G. Colombo 3,  
I-35131 Padova, Italy  
Fax: +39 049 827 6300  
Tel: +39 049 827 6337  
E-mail: beltmar@civ.bio.unipd.it

(Received 25 January 2005, revised 7  
February 2005, accepted 28 February 2005)

doi:10.1111/j.1742-4658.2005.04634.x

The hemocyanin of the tiger shrimp, *Penaeus monodon*, was investigated with respect to stability and oxygen binding. While hexamers occur as a major component, dodecamers and traces of higher aggregates are also found. Both the hexamers and dodecamers were found to be extremely stable against dissociation at high pH, independently of the presence of calcium ions, in contrast to the known crustacean hemocyanins. This could be caused by only a few additional noncovalent interactions between amino acids located at the subunit–subunit interfaces. Based on X-ray structures and sequence alignments of related hemocyanins, the particular amino acids are identified. At all pH values, the  $p_{50}$  and Bohr coefficients of the hexamers are twice as high as those of dodecamers. While the oxygen binding of hexamers from crustaceans can normally be described by a simple two-state model, an additional conformational state is needed to describe the oxygen-binding behaviour of *Penaeus monodon* hemocyanin within the pH range of 7.0 to 8.5. The dodecamers bind oxygen according to the nested Monod–Whyman–Changeaux (MWC) model, as observed for the same aggregation states of other hemocyanins. The oxygen-binding properties of both the hexameric and dodecameric hemocyanins guarantee an efficient supply of the animal with oxygen, with respect to the ratio between their concentrations. It seems that under normoxic conditions, hexamers play the major role. Under hypoxic conditions, the hexamers are expected not to be completely loaded with oxygen. Here, the dodecamers are supposed to be responsible for the oxygen supply.

The oxygen transport proteins hemocyanins (Hcs) are present in the hemolymph of molluscs and arthropods as high-molecular-weight oligomers. The biological function of this protein is based on the equilibrium shift between a low-affinity (deoxy-Hc) and a high-affinity (oxy-Hc) form that depends on the concentration of dioxygen and effectors. In arthropods, the occurrence of Hc has been well established in Crustacea, Chelicerata and Myriapoda [1–3]. Meanwhile, extending the screening to different taxa has demonstrated a wider distribution of Hc as an oxygen carrier [4–6].

The basic structure of all arthropod Hc oligomers is a hexamer of subunits [7]. This structure has been solved by crystallography [8,9] and by electron and cryoelectron microscopy [10–12], allowing for a precise definition of the intersubunit interactions. The hexamer is organized in two layers that are rotated with respect to each other and include three subunits each. A threefold symmetry axis connects the subunits along the axial position of the molecule, whereas six twofold symmetry axes, running perpendicular to the threefold axis, connect the subunits belonging to different layers.

## Abbreviations

Hc, hemocyanin;  $h_{50}$ , Hill-coefficient at half-saturation; MWC, Monod–Whyman–Changeaux;  $p_{50}$ , oxygen partial pressure at half-saturation; SS, squared residuals.

The arthropod Hc subunits are polypeptide chains folded into three domains where the active site, formed by 'domain 2', is deeply buried in the protein fold. Six histidines, belonging to a four antiparallel  $\alpha$ -helices motif, represent the ligands for two copper ions that are fundamental for the binding of dioxygen. The availability of several subunit sequences [13] of the crystallographic structure of two deoxy-Hcs (*Panulirus interruptus* a and b subunits [9]; *Limulus polyphemus* subunit II [8]), and of one oxy-Hc (*L. polyphemus* subunit II [14]), have provided important information on the structural basis for the oligomerization and for the conformational changes occurring upon the binding of dioxygen.

The hexameric aggregate represents the building block for further oligomerization to the  $2 \times 6$ -meric,  $4 \times 6$ -meric,  $6 \times 6$ -meric and  $8 \times 6$ -meric aggregates [3]. This aggregation depends on the presence of specific subunits that act as 'linkers' between hexamers, providing the correct pairing of intrahexamers contact areas. The highly conserved tertiary fold among arthropod Hcs, and the elucidation of primary structures, allows for tracing the putative structures of the oligomers by homology modelling, as accomplished for the  $4 \times 6$ -meric tarantula Hc [15]. Subunit heterogeneity has also been correlated with modulation of the oxygen-binding properties of Hcs [16–19] and, at least in some cases, it seems to be involved in adaptative mechanisms in response to environmental stimuli [20–23].

The active site of deoxy-Hc is a colourless di-Cu(I) complex. Oxygen binding occurs via a two-electron transfer from copper to oxygen, the resulting complex is described as a  $\mu:\eta^2-\eta^2$  Cu(II)–peroxide complex [24]. This complex represents an important chromophore that reports on the concentration of oxy-Hc as it exhibits an intense peroxide-to-Cu(II) charge transfer band at  $\approx 340$  nm ( $\epsilon \approx 18\,000$  M<sup>-1</sup>·cm<sup>-1</sup>) [25]. It seems that the cooperative and allosteric oxygen-binding behaviour of hexamers can often be described by the simple, two-state Monod–Whyman–Changeaux (MWC) model [26], whereas higher aggregation levels require more extended models. A characteristic feature of arthropod Hc oligomers is the increase of cooperativity with increased aggregation state [3,27] and highly hierarchical allosteric interactions, such as those involved in the 'nested' MWC model [28–30]. Information about the structural differences of the different conformations involved in the establishment of cooperative behaviour has also recently been obtained by small angle X-ray scattering. In the case of the  $4 \times 6$ -meric tarantula Hc, all protein structural levels are involved in the conformational transition upon oxygenation [31,32]. Furthermore, data obtained in the absence and

presence of the allosteric effector, lactate, showed that the interhexameric distance in the dodecameric *Homarus americanus* Hc is shortened by 1.1 nm upon lactate binding [33]. It is also worth noting that the homohexamers, prepared by reassociating homogeneous preparations of a given subunit, exhibit an oxygen-binding affinity which is lower than that of the native protein, again pointing to the importance of a correct subunit pattern for fulfilling the physiological role [18,27,34].

There is an increasing interest in characterizing the structural stability of arthropod Hc oligomers, the reversibility of the dissociation processes and the occurrence of different subunits, in order to correlate the structural properties of the various aggregation forms with their oxygen-binding properties. The ultimate aim is a precise definition of the allosteric unit responsible for cooperativity and of the possible role of heterogeneity at subunit level in the modulation of the functional properties [18,27,34].

In this article we focused on the Hc isolated from the prawn, *Penaeus monodon*. This species is interesting from an evolutionary point of view as peneid shrimps represent the ancestral branch of all Decapoda [35]. The oligomers of this protein exhibit an unusually high stability that can be rationalized in terms of available information on the stabilizing forces by homology modelling of another *Penaeus* sequence. Furthermore, the oxygen-binding properties were also studied to determine whether the unusually strong intersubunit interactions that stabilize the hexamers can be correlated with the allosteric properties of the protein and to trace the evolutionary pathway of the allosteric behaviour.

## Results

### Characterization of the oligomeric state of *P. monodon* Hc

In gel-filtration experiments of native *P. monodon* Hc, two peaks were obtained at pH 7.5 in the presence of Ca<sup>2+</sup> (Fig. 1). The first peak (Fig. 1, peak A) corresponds to dodecameric Hc, while the second (Fig. 1, peak B) represents the hexameric form, based on the column calibration with *Carcinus aestuarii* Hc. The elution pattern does not change upon removal of Ca<sup>2+</sup> ions by EDTA (data not shown). This is in contrast to many other crustacean Hcs, where the dodecameric form represents the most abundant species in the presence of divalent cations at neutral pH, but dissociates into hexamers in the absence of divalent ions [3]. This characteristic is shared also by other Hcs of the genus

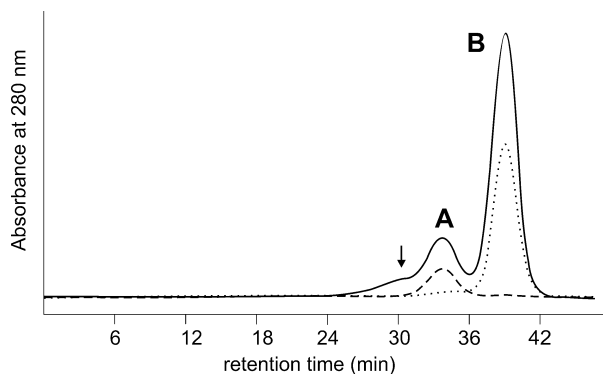


**Fig. 1.** Analysis of the aggregation state of *Penaeus monodon* hemocyanin (Hc). Gel filtration chromatography (Superose 6H 10/30) of native Hc was carried out in 50 mM Tris/HCl, 20 mM CaCl<sub>2</sub>, pH 7.5 (solid line). The dashed line and the dotted line indicate the elution profile of a further chromatography of the material included in peak A and peak B, respectively. The arrow identifies the broadening of the profile at lower elution volumes caused by higher molecular mass material.

*Penaeus*, such as *P. semisulcatus* and *P. japonicus* (M. Beltramini, unpublished results). The observed elution pattern does not result from equilibrium between the two aggregation states, as rechromatography of the individual peaks shows only the peak corresponding to the selected aggregation form (Fig. 1). The dodecameric Hc peak shows a shoulder at lower elution volumes, indicating the presence of high-molecular-weight aggregates (Fig. 1, arrow). Therefore, this peak was subjected to preparative gel chromatography and analysed by native PAGE. The results are shown in Fig. 2,

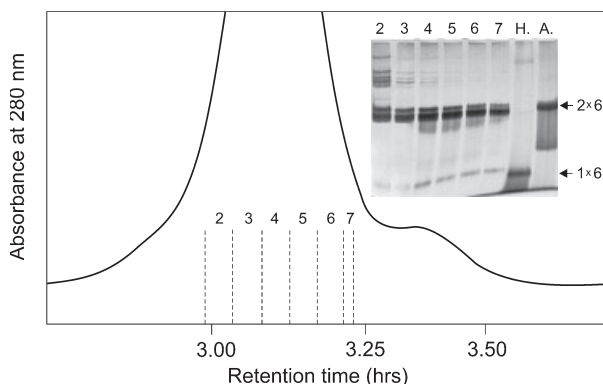


**Fig. 2.** Analysis of the oligomeric state of *Penaeus monodon* hemocyanin (Hc). Preparative gel filtration chromatography and PAGE (inset) of dodecameric Hc. The dashed sections 2–7 identify specific fractions that are collected and analysed by native PAGE at pH 7.5 (inset). The Hc from *Homarus americanus* (H) and *Astacus leptodactylus* (A) are used as markers for the hexameric (1 × 6) and dodecameric (2 × 6) aggregation state, respectively. A Fractogel XK 26/100 preparative grade column was eluted with 50 mM Tris/HCl, 20 mM CaCl<sub>2</sub>, pH 7.5.

where PAGE reveals the presence of several types of oligomers above the dodecameric level causing the leading edge shoulder (Fig. 2, inset). The shoulder eluting between 3.25 and 3.50 h represents a small fraction of hexameric Hc still present after collection and was not further analysed.

The native *P. monodon* Hc pool shows, when analyzed by SDS/PAGE, two bands with 67 and 65 kDa components, either with or without dithiothreitol treatment, indicating that disulphide bridges are not involved in the formation of the quaternary structure.

In order to further characterize the aggregation states of *P. monodon* Hc, the material eluting as fractions 2 and 6 in the preparative chromatography of Fig. 2 was analyzed by light scattering (Fig. 3). In Fig. 3A the distribution of molar mass in the elution

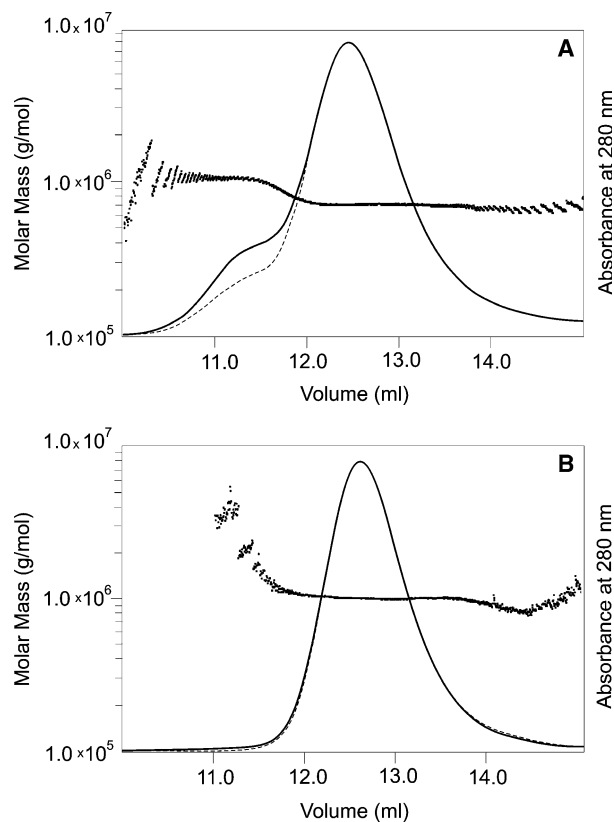


**Fig. 3.** Analysis of the oligomeric state of *Penaeus monodon* hemocyanin (Hc): gel-filtration chromatography and light scattering determination of molar mass. Specific fractions of dodecameric Hc, prepared as described in Fig. 2, were further fractionated through Superose 6HR 10/30 in 50 mM Tris/HCl, 20 mM CaCl<sub>2</sub>, pH 7.5, and the molar mass of the eluted material is determined by light scattering, as described in the Experimental procedures. (A) and (B) show the results obtained with fractions 2 and 6 of Fig. 2, respectively. The solid and dashed lines represent the elution profiles as traced following the absorbance at 280 nm and the light scattering, respectively.

profile obtained from fraction 2 is shown. The elution profile indicates the existence of two species: one minor component with a molecular mass of  $\approx 1.8 \times 10^6$  Da and a major component of  $\approx 0.95 \times 10^6$  Da. It is worth noting that the results do not change when Hc is incubated and eluted with 10 mM EDTA, proving that the aggregation states do not depend on the presence of divalent cations. The molecular mass value may indicate the presence of  $4 \times 6$ -meric molecules in the fraction corresponding to the front shoulder (Fig. 1, arrow). In contrast, the elution of fraction 6 is nearly homogenous, yielding a molecular mass of 0.95 mDa, as would be expected for a 12-meric Hc. Only slight contamination with a hexameric species is visible (above 14 mL), which is in agreement with the results of PAGE in Fig. 2.

The heterogeneity of the dodecameric Hc is manifested also by the ion-exchange chromatography experiments at different pH values in the presence of EDTA. The dodecameric Hc peak broadens as the pH of the solution increases. This broadening indicates heterogeneity in the dodecamers, rather than dissociation to hexamers, as gel filtration at pH 9.2 does not show the formation of a dominant population of hexamers, even at prolonged incubation (see below). In contrast, the elution profile of hexameric Hc is not modified upon pH changes. The same behaviour for both oligomers is observed in the presence of  $\text{Ca}^{2+}$  ions, in agreement with the observation that also the pattern of oligomers is not affected by calcium (data not shown).

### Stability of the oligomeric state

Typically, arthropod Hcs can be dissociated into subunits under non-denaturing conditions by removing divalent cations with EDTA and increasing the pH. The dodecameric Hc from *P. monodon* is found to be rather stable because the gel-filtration pattern after 48 h of incubation at pH 9.2 in the presence of 10 mM EDTA shows the persistence of the dodecameric aggregation state (Fig. 4A, peak a) with the appearance of only a small fraction of the hexameric form (Fig. 4A, peak b) and of monomers (Fig. 4C, peak c). At prolonged incubation (216 h), mainly a further peak (d), eluting later, is increasing, whereas the relative size of the peaks a, b and c remain constant (Fig. 4B). The assignment of peaks b and c is based on the well-established elution pattern of hexameric and monomeric *C. aestuarii* Hc [34] (Fig. 4C). The sharp peak d may derive from a slow pH-induced fragmentation of the protein. Increasing the pH to 11.5 results in a very complicated elution pattern and the peaks cannot be attributed to any discrete native-like structures (data

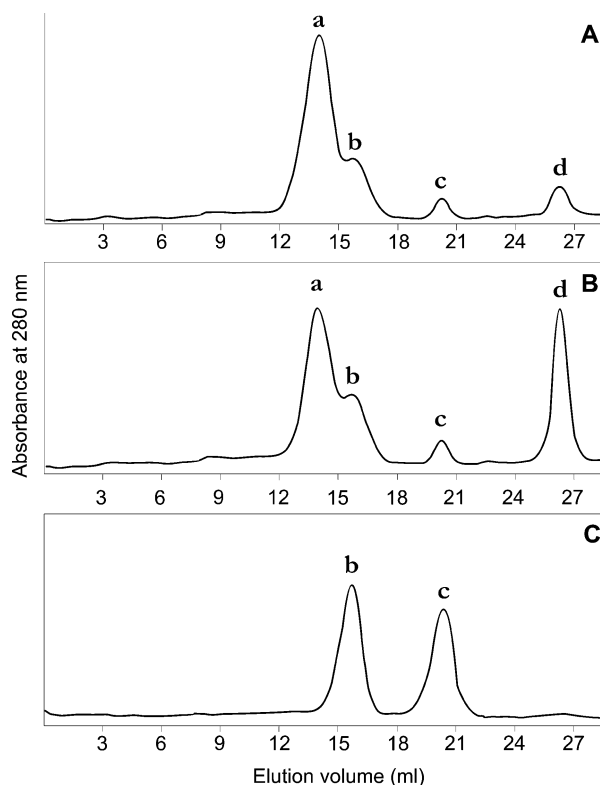


**Fig. 4.** Alkaline dissociation of *Penaeus monodon* hemocyanin (Hc). Gel filtration of the dodecameric Hc fraction eluted on a Superose 6H 10/30 analytical column equilibrated with 50 mM Tris/HCl, 10 mM EDTA pH 9.2, after 48 h (A) and 216 h (B) of incubation in the same buffer. The Hc of *Carcinus aestuarii*, eluted under the same conditions, was used as a marker for the hexameric and monomeric states. The letters identify dodecameric (a), hexameric (b), monomeric (c) Hc and low molecular mass fragments (d).

not shown). The hexameric form does not change its aggregation state upon 48 h of incubation at pH 9.2 with 10 mM EDTA, but it dissociates at pH 11.5, as observed with the dodecameric form (data not shown).

As it was not possible to produce well-defined dissociation products upon treatment with EDTA and increased pH, the effects of increasing concentrations of NaSCN and  $\text{NaClO}_4$  were studied. The first salt is a powerful protein denaturant, whose behaviour in aqueous solutions has been investigated in detail [36]. The second is a salt close to  $\text{NaClO}_4$  in the chaotropic Hofmeister's series that proved to affect protein folding and induce protein denaturation [37–39]. To follow the capability to bind oxygen, the absorbance ratio at 340 and 280 nm ( $A_{340}/A_{280}$ ) was measured. These experiments were carried out in 50 mM Tris/HCl, 10 mM EDTA, at either pH 7.5 or 9.5 (Fig. 5). Increasing concentrations of perturbant results in a sigmoid curve typical for a two-state transition. Up to 300 mM

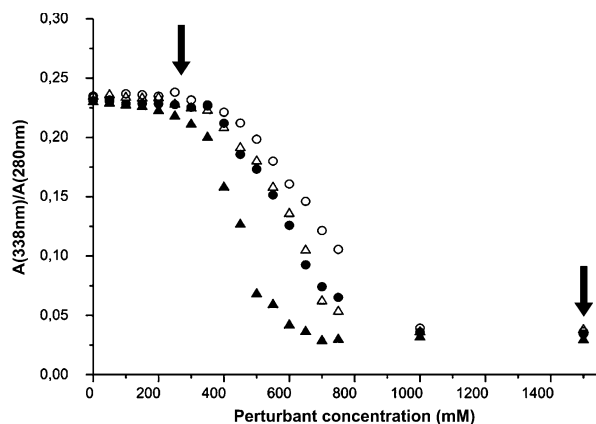


**Fig. 5.** Stability of *Penaeus monodon* hemocyanin (Hc) as a function of conformation perturbants. The oxygenation state ( $A_{340}/A_{280}$ ) was measured at different concentrations of  $\text{NaClO}_4$  (●,○) and of  $\text{NaSCN}$  (▲,△) at pH 7.5 (filled symbols) and pH 9.5 (empty symbols). The buffer used was 50 mM Tris/HCl, 10 mM EDTA, at the indicated pH. The arrows indicate the concentrations of perturbants used to check the aggregation state by gel filtration chromatography (Fig. 7).

perturbant, the  $A_{340}/A_{280}$  ratio remains constant at 0.21 (corrected for the spectral background after complete disappearance of the oxy-Hc band), indicating that Hc remains fully oxygenated. Thus, the 0–300 mM region defines the concentration range suitable for carrying out gel filtration experiments to analyse the quaternary structure of the protein under conditions where active sites still bind oxygen. The results of a gel filtration analysis at 300 mM  $\text{NaSCN}$ , as reported in Fig. 6B, demonstrate that the protein is still in the oligomeric form, indistinguishable from the protein in the absence of perturbant (Fig. 6A), with the exception of a slight increase of retention time that can be attributed to a change in the hydrodynamic radius of the protein in the presence of a high salt concentration. At a higher perturbant concentration of 1.5 M  $\text{NaClO}_4$ , where the absorption band is abolished, a remarkable modification of the elution pattern occurs (Fig. 6C). Under these conditions, the fluorescence emission spectra (excitation either 280 or 294 nm, data not shown) have maxima at  $\approx 345$  nm, red shifted with respect to the protein in the absence of perturbants (emission maximum at  $\approx 330$  nm). These results point to denaturation of the protein, and hence no attempt to further characterize the various aggregation state(s) was made.

### Sequence alignment and homology studies

The stability of the oligomeric structure towards removal of divalent ions seems to be a characteristic feature of the genus *Penaeus*. This suggests that

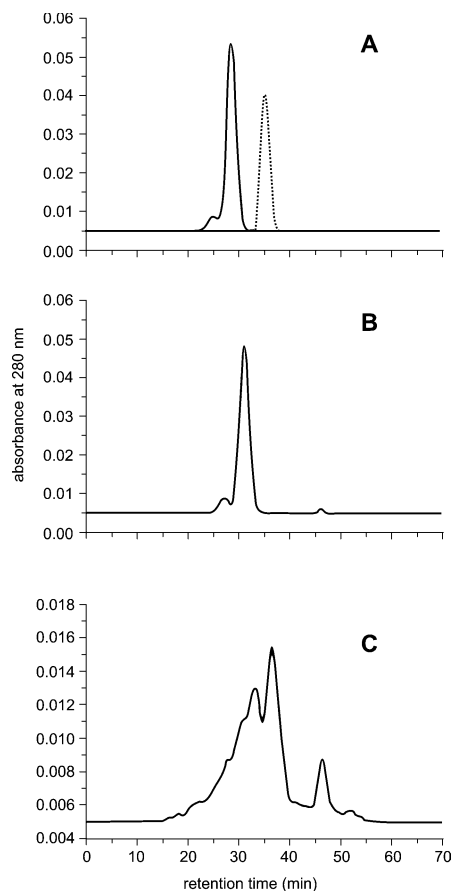


**Fig. 6.** Stability of *Penaeus monodon* hemocyanin (Hc) at different concentrations of chaotropic solutes. Gel filtration of the native Hc eluted on a Superose 6H 10/30 analytical column equilibrated with 50 mM Tris/HCl, 10 mM EDTA, pH 9.5. (A) Buffer alone; (B) buffer containing 300 mM  $\text{NaClO}_4$ ; (C) buffer containing 1.5 M  $\text{NaClO}_4$ . The monomeric fraction of *Carcinus aestuarii* Hc, eluted under the same conditions, was used as marker (dotted line in A).

genus-specific changes in the amino acid sequence should be determined, specifically at those positions which are likely to be involved in the formation of the quaternary structure. As the amino acid sequence is available only for *P. vannamei* Hc [40], we used this species for an alignment of the primary structure with other Hc sequences, which dissociate under 'standard' stripping conditions, namely removal of  $\text{Ca}^{2+}$  ions and increasing pH, but retain the oxygen-binding property as well as the capability to reassociate [3]. The high sequence similarity within crustacean Hcs (50–92% [13]), in general, and the observation that the high structural stability is a common feature within the genus *Penaeus*, allow this strategy. The areas putatively involved in subunit contacts were deduced from the X-ray crystallographic map obtained for the *Pan. interruptus* hexamer composed of subunits



**Table 2.** Amino acids involved in the pairwise interactions in areas 1 and 2 of tight contact between dimers, as shown from X-ray crystallography of *Panulirus interruptus* sub. A and multiple alignment (Table 1). Hc, hemocyanin.

Hc species	Areas of tight dimers contact and residues involved				
	Area 1				Area 2
	155/159	159/438	160/439	160/438	177/360
<i>Panulirus interruptus</i> sub A	Tyr-Met	Met-Asp	Thr-Ser	Thr-Asp	Arg-Lys
<i>Panulirus interruptus</i> sub B	Tyr-Met	Met-Asp	Thr-Ser	Thr-Asp	Arg-Lys
<i>Panulirus interruptus</i> sub C	Tyr-Met	Met-Asp	Thr-Asp	Thr-Asp	Pro-Lys
<i>Callinectes sapidus</i>	Tyr-Met	Met-Asp	Thr-Asp	Thr-Asp	Pro-Lys
<i>Cancer magister</i>	Tyr-Met	Met-Asp	Thr-Asp	Thr-Asp	Pro-Lys
<i>Palinurus elephas</i>	Tyr-Met	Met-Asp	Thr-Ser	Thr-Asp	Lys-Lys
<i>Palinurus vulgaris</i> sub 1	Tyr-Met	Met-Asp	Thr-Ser	Thr-Asp	Lys-Lys
<i>Palinurus vulgaris</i> sub 3	Tyr-Met	Met-Asp	Thr-Ser	Thr-Asp	Lys-Lys
<i>Palinurus vulgaris</i> sub 2	Tyr-Met	Met-Asp	Thr-Ser	Thr-Asp	Arg-Lys
<i>Palinurus vulgaris</i>	Tyr-Met	Met-Asp	Thr-Ser	Thr-Asp	Arg-Lys
<i>Homarus americanus</i>	Tyr-Met	Met-Asp	Thr-Glu	Thr-Asp	Lys-Lys
<i>Pontastacus leptodactylus</i>	Tyr-Met	Met-Asp		Thr-Asp	Lys-Lys
<i>Pacifastacus leniusculus</i>	Tyr-Met	Met-Asp	Thr-Thr	Thr-Asp	Arg-Lys
<i>Penaeus vannamei</i>	Tyr-Gln	Gln-Asp	Lys-Asp	Lys-Asp	Pro-Lys

following analysis we refer to sequence Q26180, CAA57880, although the considerations regarding Lys(Thr)160 need to be confirmed by further sequence studies within *Peneidae*.

The sequence positions reported in Table 2 include amino acids that are involved in tight dimer contact areas in the hexamer of *Panulirus* Hc. The corresponding amino acid positions in *P. vannamei* were identified based on the assumption that it is a homo-hexamer. Out of a total of 19 tight dimer contacts and 12 trimer contacts, we have selected the five positions indicated in Table 2 because they are occupied by different residues in *Penaeus* Hc and might change the interaction pattern compared with *Panulirus* Hc. In particular, in the area 1 of tight dimer contacts, the substitution of the Tyr155–Met159 pair (in *Panulirus* Hc) with Tyr155–Gln159 (in *Penaeus* Hc) introduces a pair potentially capable of hydrogen bonding. This situation is specific for *Penaeus* Hc, as indicated by comparison with the other crustacean Hcs. The same is true for the substitution of the pair Met159–Asp438 (in *Panulirus* Hc) with Gln159–Asp438 (in *Penaeus* Hc). The substitution of the pair Thr160–Ser(Asp)439 in *Panulirus* Hc by Lys160–Asp439 strongly stabilizes *Penaeus* Hc because it provides an ion–ion bond. In the other crustacean Hcs, although these positions are rather variable, such a stabilizing pair does not occur. The same considerations apply also to the Thr160–Asp438 pair (in *Panulirus* and all other Crustacea) that is Lys160–Asp438 in *Penaeus* Hc. Furthermore, in the area II of tight dimers contact, the pair Arg177–Lys360 is present as Pro177–Lys360, so that a repulsive

electrostatic interaction present in *Panulirus* is absent in *Penaeus*. Interestingly, all crustacean Hc, with the exception of *Can. magister* and *Callinectes sapidus*, exhibit, in this position, repulsive interactions; *Cancer* and *Callinectes* Hc have the same structural feature as *Penaeus*. Finally, a model structural reconstruction of the *Penaeus* Hc subunit was made by modelling the sequence of *P. vannamei* Hc (SwissProt and NCBI accession numbers: Q26180, CAA57880, respectively) on the X-ray crystallographic structure of *Pan. interruptus* Hc (pdb 1HCY). In the resulting modelled structure (data not shown), the two amino acids contributing with stabilizing interactions in *Penaeus* Hc (Gln159 and Lys160), which are different in other crustacean Hcs, are indeed located in the intersubunit contact area. The same applies also to the Pro177 of *Penaeus* Hc (as well as of *Cancer* and *Callinectes*), which does not involve a repulsive interaction with Lys360, in contrast to most crustacean Hcs where Lys(Arg)177 is paired with Lys360 (Table 2). The partial sequence available for *P. monodon* Hc (accession number AF431737) does not include the region containing residues 159, 160, 177, and therefore cannot be used in the present study. However, in positions 438 and 439, two Asp residues are found, and in position 360 a Lys, as in *P. vannamei* Hc.

### Oxygen binding

Oxygen-binding curves have been determined both for the hexameric and dodecameric Hc. The data obtained for purified hexameric Hc in the pH range 7.0–8.5 are

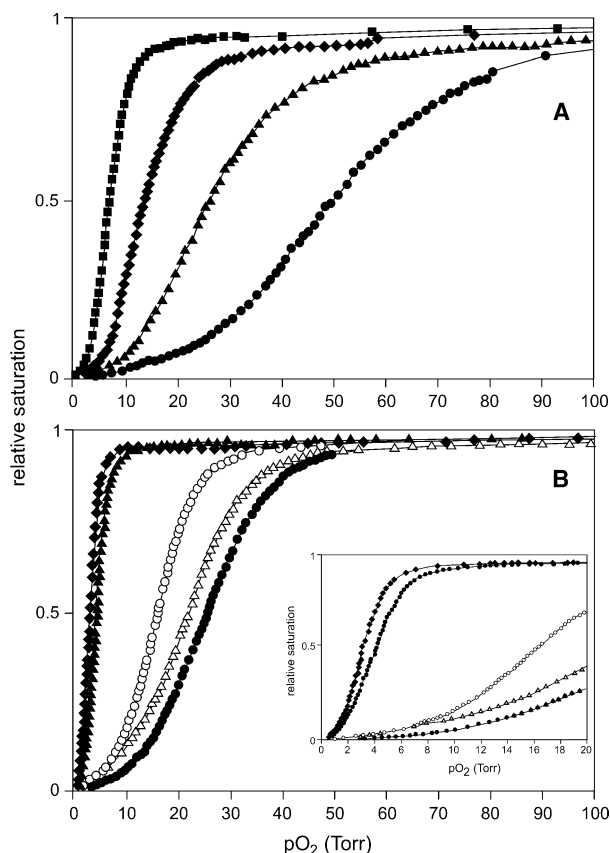


**Fig. 7.** Oxygen-binding curves of hexameric (A) and dodecameric (B) *Penaeus monodon* hemocyanin (Hc) at pH 7.0 (●), 7.2 (△), 7.3 (○), 7.5 (▲), 8.0 (◆), or 8.5 (■), in 50 mM Tris/HCl containing either 10 mM EDTA to stabilize the hexamer (A) or 20 mM CaCl<sub>2</sub> to stabilize the dodecamer (B). The inset of (B) shows the same curves in the low oxygen partial pressure range.

presented in Fig. 7A. Table 2 reports the affinity for the first and last oxygen-binding sites, the Hill-coefficient at half-saturation ( $h_{50}$ ) as well as the oxygen pressure at half saturation ( $p_{50}$ ), as determined in the Hill-Plot. The value of  $p_{50}$  decreases as the pH is increased from 7.0 to 8.5, indicating a positive Bohr effect. The Hill coefficient,  $h_{50}$ , does not change much as a function of pH. The results obtained for dodecameric Hc are presented in Fig. 7B, and the binding parameters are reported in Table 3. The oxygen affinity is much higher, and the positive Bohr effect is more pronounced, than found for the hexameric Hc. The Bohr coefficient  $\Delta \log(p_{50})/\Delta \text{pH}$  is  $-0.56$  and  $-1.05$  for hexameric and dodecameric Hc, respectively. Again, the  $h_{50}$  value is not strongly affected by pH; in contrast to the behaviour of the  $p_{50}$ , it remains essentially constant.

In order to evaluate, in greater detail, the cooperative and allosteric mechanism involved in the regulation of *P. monodon* Hc, the oxygen-binding data were analysed

**Table 3.** Oxygen-binding parameters of different oligomeric forms of *Penaeus monodon* hemocyanin (Hc) obtained from the Hill-Plot. The  $h_{50}$  represents the Hill-coefficient at half (50%) saturation.

	$p_{50}$ (Torr)	$h_{50}$	$K_T \times 10^3$ (Torr <sup>-1</sup> )	$K_R \times 10^3$ (Torr <sup>-1</sup> )
Hexameric Hc				
pH 7.0	51	3.3	3.6	122
pH 7.5	26	2.7	3.3	174
pH 8.0	14	2.9	6.0	289
pH 8.5	7	3.2	21.0	151
Dodecameric Hc				
pH 7.0	26	3.7	1.1	110
pH 7.2	23	3.4	7.4	215
pH 7.3	17	4.0	9.3	223
pH 7.5	4	3.4	66.9	524
pH 8.0	3	3.3	46.7	80

based on different concerted models for cooperativity. As, in all cases reported to date, the oxygen-binding behaviour of hexameric Hc could well be described in terms of the simple, two-state MWC model, this approach was also applied to the data shown in Fig. 7A. Indeed, oxygen-binding curves obtained at each pH value could well be described based on the MWC model when analysed individually for each pH value. However, in contrast to the expectations for the MWC model, the binding affinities for the two conformations R and T ( $K_R$  and  $K_T$ ) show a significant dependence on the pH value, ruling out this model for the whole pH range (Fig. 8A). Furthermore, the allosteric equilibrium constant,  $l_0$ , exhibits a nonmonotonic behaviour, which has not been reported for any other species to date (Fig. 8B, grey symbols). Any attempt to constrain the oxygen-binding constants to a similar value for all four data sets leads to significant deviations between fit and data. When the data at pH 8.5 are excluded from the analysis, the agreement is much better. However, there are no indications that pH 8.5 does lead to any destabilization or other perturbation, which may have suggested exclusion of these data from the analysis.

As the MWC model did not yield a satisfying description of the full pH-range, a three-state MWC model was applied to the data. This model is in very good agreement with the data, and the values for the oxygen-binding constants are fully in accordance with a concerted model. The squared residuals (SS)-value for the constrained MWC model ( $0.3 \leq k_r \leq 0.6 \text{ Torr}^{-1}$ , and  $0.004 \leq k_t \leq 0.01 \text{ Torr}^{-1}$ ) was  $\approx 0.036$ , whereas for the three-state model the SS-value was  $\approx 0.014$ . Thus, even considering that the degrees of freedom are somewhat larger for the constrained MWC, the three-state MWC gives better results.

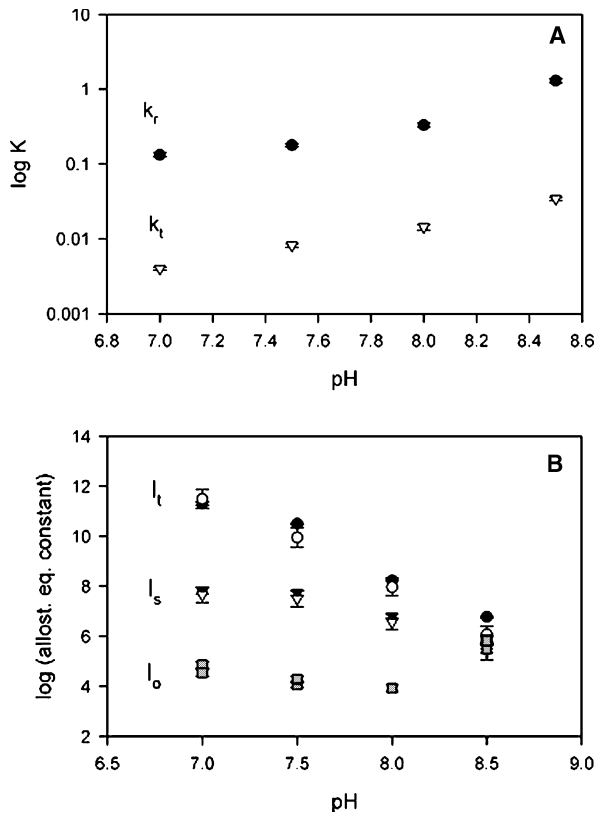


**Fig. 8.** Allosteric effect of  $H^+$  ions on hexameric *Penaeus monodon* hemocyanin (Hc) in 50 mM Tris/HCl containing 10 mM EDTA. (A) pH dependence of the oxygen-binding constants  $K_t$  and  $K_r$  resulting from the analysis based on the MWC model. (B) pH dependence of the allosteric equilibrium constants as calculated from the MWC model ( $I_o$ , grey squares) or from the three-state MWC model ( $I_s$ , triangles;  $I_t$ , circles). The empty and filled symbols refer to the two different data sets, as described in the text.

In Fig. 8B, the pH dependence of the two equilibrium constants,  $I_s$  and  $I_t$ , resulting from the three-state MWC model, are shown. For each pH value, except pH 8.0, two-binding curves (a, b) were available for the fit. As the fitting routine allows only 25 parameters to be optimized simultaneously, the binding curves were analyzed in two sets (7.0a, 7.5a, 8.0, 8.5a and 7.0b, 7.5b, 8.0, 8.5b), each including either binding curve a or b for the different pH values. The comparison of the results for the two sets shows a good agreement between all data, as demonstrated by the agreement of full and empty symbols of Fig. 8B. The oxygen-binding constants were assumed to be identical for all pH values in the analysis, and the following values were obtained:  $K_t = 0.005 \pm 0.001 \text{ Torr}^{-1}$ ,  $K_s = 0.077 \pm 0.005 \text{ Torr}^{-1}$ , and  $K_r = 1.6 \pm 0.2 \text{ Torr}^{-1}$ .

The binding data obtained for the 12-meric Hc were analysed based on the nested-MWC model, as this

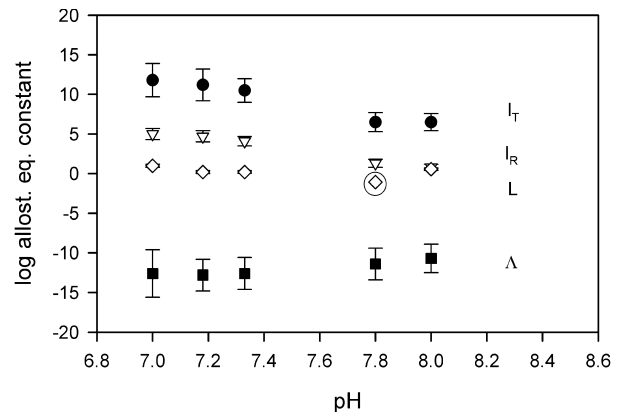


**Fig. 9.** Allosteric effect of  $H^+$  ions on dodecameric *Penaeus monodon* hemocyanin (Hc). The allosteric equilibrium constants were obtained by analysis of the data in Fig. 9B based on the nested MWC model. The allosteric equilibrium constants show a typical pH dependence ( $I_R$ ,  $\nabla$ ;  $I_T$ ,  $\bullet$ ; L,  $\diamond$ ;  $\Lambda$ ,  $\blacksquare$ ). The values for L at pH 8.0 (encircled) have a larger absolute error of  $\approx 13$ . The error bar is omitted to retain the other error bars visible.

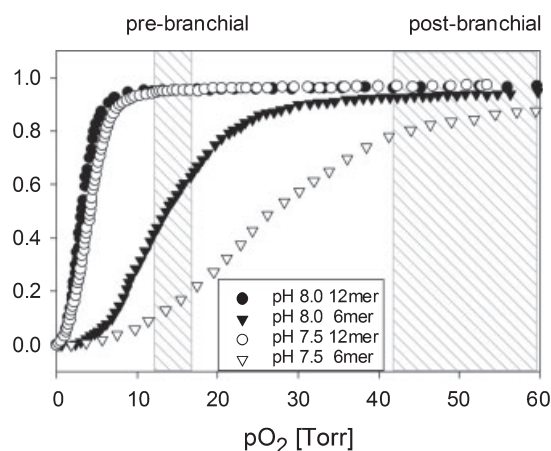
model delivered a successful description of Hc oligomers larger than hexamers for other species. This model involves a set of hierarchical interactions that are exerted within the allosteric hexameric units or within the dodecamer. Accordingly, each allosteric unit that is represented by the hexameric Hc aggregate can adopt two conformations: r and t. At the higher quaternary level, two alternative conformations, R and T, can exist for the dodecameric Hc as a whole. Thus, four different conformations can be defined as rR, tR, rT, and tT owing to the functional coupling between the two hexameric units within the dodecamer. Each conformation is characterized by an intrinsic affinity constant for oxygen ( $K_{rR}$ ,  $K_{tR}$ ,  $K_{rT}$ , and  $K_{tT}$ ), and three allosteric constants can be defined as  $I_R = [tR_o]/[rR_o]$ ,  $I_T = [tT_o]/[rT_o]$ , and  $L = [T_o]/[R_o]$ . The analysis was based on the same considerations as for the pH dependence of the oxygen-binding curves of the MWC model. The binding function for this model was fitted to several data sets simultaneously. The oxygen-binding constants were assumed to be the same for all pH values and optimized simultaneously for all data sets. Again, initially, data sets obtained at pH 7.0–7.8 were fitted simultaneously. Then, data sets obtained at pH 7.18–8.0 were analyzed in the same way. The agreement between data and fitted values is very good. The results for both runs yielded values for corresponding parameters which are the same within the error range given (Tables 4 and 5). The simultaneous fit of the curves at the different pH values reported in Fig. 7B yielded, for the different oxygen equilibrium constants, the following values:

**Table 4.** Oxygen-binding parameters of hexameric *Penaeus monodon* hemocyanin (Hc) obtained from the analysis based on the 3-State MWC model.

Hexameric Hc	log $I_T$	log $I_S$	–
pH 7.0	11.4 ± 0.4	7.7 ± 0.3	–
pH 7.5	10.2 ± 0.4	7.6 ± 0.3	–
pH 8.0	8.1 ± 0.4	6.6 ± 0.3	–
pH 8.5	6.3 ± 0.3	5.7 ± 0.3	–

**Table 5.** Oxygen-binding parameters of dodecameric *Penaeus monodon* hemocyanin (Hc) obtained from the analysis based on the nested-MWC model.

Dodecameric Hc	log $I_T$	log $I_R$	log L
pH 7.0	11.8 ± 2.1	5.0 ± 0.7	1.0 ± 0.2
pH 7.2	11.2 ± 2.0	4.7 ± 0.7	0.2 ± 0.2
pH 7.3	10.5 ± 1.5	4.1 ± 0.6	0.2 ± 0.2
pH 7.5	6.5 ± 1.2	1.3 ± 0.5	–1 ± 13
pH 8.0	6.5 ± 1.1	0.8 ± 0.4	0.6 ± 0.2

**Fig. 10.** Oxygen-binding curves of dodecameric and hexameric *Penaeus monodon* hemocyanin (Hc) (data from Fig. 9, pH 8.0 and pH 7.5) with the oxygen partial pressures of pre- and postbrachial hemolymph, expected in the case of normoxia, indicated: these values for the oxygen partial pressure are given as ranges, as found in the literature [53] for a number of different species. Based on these average values no clear distinction between hypoxic and normoxic values can be made and thus only the normoxic values are given.

$K_{iR} = 0.015 \pm 0.002 \text{ Torr}^{-1}$ ,  $K_{rR} = 0.28 \pm 0.05 \text{ Torr}^{-1}$ ,  $K_{iT} = 3 \pm 2 \text{ Torr}^{-1}$ , and  $K_{rT} \leq 0001 \text{ Torr}^{-1}$ . The pH dependence of the three allosteric equilibrium constants is shown in Fig. 9.

## Discussion

Arthropod Hcs represent a family of proteins where the quaternary organization of the oligomers originates from hexameric building blocks. Most of the interest

in structure–function studies of Hcs is now focused on the importance of the oligomeric organization for the oxygen-binding properties, with the ultimate goal being to understand their role in the adaptative strategies of arthropods.

It has been shown, in reassociation experiments, that the presence of different subunit types is essential in order to obtain quaternary structures larger than hexamers, and that different quaternary structures exhibit different cooperative and allosteric properties [18,41,42]. Furthermore, the different subunit types also play a role in the homotropic and heterotropic interactions. As an example, we have shown that the homo-hexamers obtained by reassociating a single subunit of king crab (*Paralithodes camtschaticae*) Hc have much lower oxygen affinity than the native hexamer or with hexamers obtained by reassociating a pool of subunits [19]. Several *in vivo* experiments have demonstrated that environmental stimuli affect the expression of certain subunits of *Cal. sapidus* Hc, hence affecting the oxygen affinity of the circulating oligomer [41]. In the case of *Astacus astacus*, the dodecamer/hexamer ratio is shifted by adaptation to different temperatures [42]. This structural and functional plasticity is believed to play an important role in the physiological adaptation of crabs to environmental changes [23].

The hemolymph of the tiger shrimp, *P. monodon*, contains a predominant Hc component with a hexameric aggregation state, which is homogeneous both in electrophoresis and ion-exchange chromatography. Further components can be identified as dodecameric, and traces of  $4 \times 6$ -meric molecules have been found on the basis of the gel filtration/light scattering experiments. It is worth noting that only these low concentration aggregates are heterogeneous, as deduced from PAGE and ion-exchange chromatography. An unusually high stability has been reported for Hc from *P. setiferus*, for which dissociation of the protein was observed only in concomitance with the loss of oxygen-binding properties, thus under denaturing conditions [43]. Our study of Hc from *P. monodon* revealed a very similar behaviour. The oxygen-binding ability, measured as  $A_{340}/A_{280}$ , remained unaltered up to 300 mM salt of chaotropic Hofmeister's series. A further increase of salt concentration leads to a decrease of the oxygenation level together with a red shift of the intrinsic tryptophan fluorescence emission maximum. Such effects are fully compatible with a concomitant oxygen dissociation and denaturation of Hc. The sigmoidal plot of  $A_{340}/A_{280}$  vs. salt concentration can be interpreted in terms of a conformational transition between a native oligomeric state and an unfolded state, following a model previously applied to the Hc

of the brachiuran crab *Car. aestuarii* [44,45]. In line with this interpretation are the gel-filtration experiments in the presence of Hofmeister's salts in which, under conditions that do not modify the  $A_{340}/A_{280}$  ratio, the elution pattern does not change compared with the nondissociating conditions. At the higher salt concentration, under denaturing conditions, a peak corresponding to monomeric Hc is observed; however, the elution profile is complicated by a broadening to the high-molecular-weight region, suggesting the formation of aggregated 'misfit' material that includes unfolded molecules. Thus, it seems that for *P. monodon*, Hc dissociation of the oligomers can be achieved only under denaturing conditions. Therefore, a study on the oxygen-binding properties of isolated monomer or reassociated homo- or hetero-hexamers (as carried out with other brachiuran crab Hcs [19,34]) is precluded. A very low sensitivity towards removal of  $\text{Ca}^{2+}$  and high pH has also been found for Hc from *P. semisculatus* and *P. japonicus* (M. Beltramini, unpublished work). These observations suggest that investigations should be carried out for characteristic changes in the amino acid sequence in *Penaeus* Hc, which might account for the high stability of this species.

A possible approach to rationalize the high stability of *Penaeus* Hc is to carry out an analysis of the amino acid substitutions in *Penaeus* Hc, in comparison to less stable Hcs, and to interpret the results based on known X-ray structures. For this purpose, the sequence of *P. vannamei* Hc was used, because, to date, that of *P. monodon* has not been fully determined. This sequence was compared to sequences of other Hcs that all dissociate under typical dissociating conditions. Among those residues that may be involved in intersubunit interactions within hexamers, only a few are substituted in Hc from *P. vannamei*, possibly leading to the increased stability found in the other *Penaeus* Hcs: the 159Gln–438Asp and 159Gln–155Tyr H-bonds, together with the absence of repulsive interaction 177Pro  $\times$  360Lys (Table 2). These structural features appear to be characteristic signatures of *P. vannamei* Hc because they are not present in other crustacean Hcs (Table 2). The 160Lys–438Asp and 160Lys–439Asp ion–ion interactions need to be confirmed by further sequence studies within the peneid Hcs, as pointed out above. As peneid shrimps represent the ancestral branch of all Decapoda, it seems that during evolution the ability to form very stable aggregates was lost in other Crustacea owing to the above-mentioned substitutions. The other positions involved in interhexameric interactions remained functionally unchanged, guaranteeing the formation of the oligomeric structure under appropriate conditions. On

these positions, a selective pressure has been exerted because, in order to establish cooperativity in oxygen binding, oligomerization is necessary. These positions can be identified by the strict conservation of the chemical features of amino acids listed in Table 1, C or I, and, to some extent, also I\* and C\*. The lower stability of Hc from nonpeneid Crustacea yields a structure where divalent ions (such as  $\text{Ca}^{2+}$  and  $\text{Mg}^{2+}$ ) and pH regulate the oligomerization state. It seems that the high stability is more crucial for *Penaeus* Hc than the possibility of additional means of regulation.

The sequence alignment shows that a number of positions, likely to be involved in subunit interactions, are functionally conserved. The alignment is based on different subunit types that are not likely to occupy all the same positions within a hexamer. Thus, for a discussion of these interactions, a homo-hexamer yields the same results as any hetero-hexamer. With respect to those residues, which are changed in the sequence of Hc from *P. vannamei* in comparison to the other Hcs, it cannot be excluded that part of the identified changes are subunit-type specific. They could be sporadic substitutions, similarly to those identified in the comparison of the other Hcs. However, the sporadic substitutions, as discussed, occur only at one position, whereas for Hc from *P. vannamei* several changes are found. Thus, it is probable, albeit not proven, that these changes are specific for the genus *Penaeus*.

Does this particular stability of *P. monodon* Hc have some special consequence for its functional properties? In contrast to other hexameric Hcs [19,26,34,46], the oxygen-binding data for the hexameric *P. monodon* Hc cannot be described using the simple MWC model. This is based on the following considerations: when applying concerted models for cooperativity, it is assumed that certain conformations exist that are characterized by their affinity for ligands (here oxygen) and effector (here protons). Thus, changing the pH should not have an effect on the values for the oxygen-binding constants for the conformations R and T, as postulated for the MWC model. However, the analysis showed a remarked pH dependence when analyzed without any constraints. Furthermore, the allosteric equilibrium constants exhibit a nonmonotonous dependence on pH. From a theoretical point of view this is possible, but has not been observed, to date, for any Hc. We tried to constrain the values for the oxygen-binding constants, forcing them to be similar for all pH values. However, this always led to increasing sums of squared residuals (SS). An analysis including a third conformation, yielding a three-state MWC model, gave much better results, similarly to the model

including a symmetrical hybrid state,  $R_3T_3$ , that has been postulated for *P. setiferus* Hc [43]. A three-state MWC model was also used for Hcs larger than hexameric Hc [47,48].

The dodecameric Hc of *P. monodon* can be analyzed based on the nested MWC model, similarly to a number of other 12- or 24-meric Hcs [49]. Furthermore, the values for the allosteric equilibrium constants show the same type of pH-dependence as seen with other Hcs, where the nested-MWC model is applicable [30]:  $L$  (as calculated from  $\Lambda$ ,  $l_T$  and  $l_R$ ) does depend only weakly on pH, whereas  $l_T$  and  $l_R$  exhibit a significant pH-dependence. The values for the oxygen-binding constants also show the typical pattern  $k_{lT} < k_{lR} < k_{rR} < k_{rT}$ . The dodecamer of *P. monodon* Hc exhibits a somewhat stronger Bohr effect [ $\Delta \log(p_{50})/\Delta \text{pH} = -1.05$ ], than the hexameric form of the same species ( $-0.56$ ) or the hexamer from other Hcs isolated from crustaceans living under normoxic conditions: values of  $-0.70$ ,  $-0.83$ ,  $-0.57$ , and  $-0.68$  have been measured for *Can. pagurus*, *Car. maenas* [50,51] *Par. camtschaticae* [19] and *Car. aestuarii* [34], respectively. In contrast, crustaceans living under hypoxic conditions, such as the deep-sea hydrothermal vent crab, have a Hc with a large Bohr-effect of  $-1.80$  [52]. For Hc from *P. monodon*, at each pH value the mean oxygen affinity,  $p_{50}$ , of the hexamer is lower than that of the dodecamer. In contrast, for the Hc from *Ast. astacus*, the hexamer exhibits a higher oxygen affinity [41]. Similarly, the affinity of Hc from *Eurypelma californicum* decreases with increasing oligomerization state [27]. In *P. monodon* Hc, this higher aggregate form represents only a minor part of total Hc, thus most of the oxygen transport/delivery is exerted by the hexameric Hc whose Bohr effect is comparable with that of crustaceans adapted to normoxic waters. Figure 10 shows oxygen-binding curves of dodecameric and hexameric *P. monodon* Hc with indications of the oxygen partial pressures of pre- and postbranchial hemolymph expected in the case of normoxia. The shaded areas are deduced from values reported for a number of Hcs [53]. *P. monodon* is adapted to water conditions where the temperature does not change markedly. Thus, the oxygen solubility is not externally altered, the availability of oxygen does not exert a selective pressure, and the hexameric form with its lower overall affinity is sufficient to ensure full oxygenation. Furthermore, it seems that the 12-meric species is deoxygenated only minimally under typical conditions. However, as no species-specific information about post- and prebranchial oxygen concentrations are available for *P. monodon*, situations might exist where the properties of the dodecameric form are important. It is possible that the relative dodecamer-to-hexamer

concentration ratio is controlled by environmental conditions (i.e. temperature, or oxygen partial pressure).

In summary, hexameric Hc from *P. monodon*, which is dominant in the hemolymph, differs from other crustacean Hcs in the following aspects: (a) it is very stable towards the removal of divalent ions and increase in pH; and (b) its oxygen-binding properties cannot be described by a simple two-state MWC model, in contrast to all other hexameric forms described to date. Furthermore, the hexameric Hc exhibits a higher stability and lower oxygen affinity than the dodecameric oligomer, while usually the higher aggregated forms are more stable and have a lower affinity. The emerging picture therefore is as follows: interaction levels above the simple two-state MWC model are apparently evolved also in *P. monodon* to ensure a fine tuning of the allosteric behaviour involving effectors ( $H^+$ ) and ligand ( $O_2$ ). Given that the hexameric molecule is the dominant aggregation state in this species, it seems plausible that the plasticity of the molecule is enhanced by creating a third conformation in order to allow for this fine tuning. However, it remains unclear why the dodecamers did not evolve as the prevailing species, as demonstrated in other Crustacea where more than one aggregation state of Hc was found.

## Experimental procedures

### Isolation and purification of Hc

*P. monodon* Hc was isolated from the hemolymph obtained from living specimens, kindly provided by the aquaculture plant 'Biotopo Bonello' (ESAV, Porto Tolle (RO), Italy). The hemolymph was collected via a syringe injected in the dorsal lacuna. Typically, a volume of  $\approx 1$ – $2$  mL of hemolymph was collected from 20–35 g of specimens. In order to limit hemolymph clotting, 100–200  $\mu\text{L}$  of a buffered 1% (w/v) sodium citrate solution in 50 mM Tris/HCl, pH 7.5, was injected before collecting the sample. For small individuals, an alternative procedure for bleeding was preferred: the exoskeleton and muscles in the intersegmental regions were cut and the hemolymph was obtained by gentle squeezing. The extracted material was filtered through gauze and the hemolymph was adjusted to 50 mM in  $\text{NaH}_2\text{PO}_4$ . The solution was then dialysed overnight against 50 mM Tris/HCl, 20 mM  $\text{CaCl}_2$ , pH 7.5. The precipitation of calcium phosphate in the hemolymph solution results in the adsorption of lipids and carotenoids that are removed by centrifugation at 23 700 g, 4 °C, 20 min in a Beckman centrifuge (model J2-21). The supernatant solution was dialysed against 50 mM Tris/HCl, 20 mM  $\text{CaCl}_2$ , pH 7.5, centrifuged (as described above) to eliminate possible precipitates, and sedimented in a Beckman centrifuge (model XL-70, rotor 70ti, 4 °C) at 295 807 g for 4 h. The pellet was redissolved in 50 mM

Tris/HCl, 20 mM CaCl<sub>2</sub>, pH 7.5 and sedimented again. Finally, Hc was resuspended in this buffer, and 20% (w/v) sucrose was added to the solution, which was then stored at -20 °C until used.

The protein concentration was determined spectrophotometrically using an extinction coefficient of  $74\,100 \pm 2000\text{ M}^{-1}\text{cm}^{-1}$  at 278 nm based on the monomer concentration. This value was established by correlating the absorbance at this wavelength with the copper content of the solution determined either by atomic absorption spectroscopy (Perkin-Elmer Analyst 100 spectrometer), using the internal standard method [54], or the colorimetric assay, using 2,2' biquinoline [55], with addition of excess hydroxylamine to reduce copper.

The content of oxy-Hc in the protein samples was determined by measuring the absorbance ratio,  $A_{340}/A_{278}$ , and considering the value of 0.21 for a solution containing 100% oxy-Hc. Fluorescence spectra were recorded on a Perkin-Elmer (Wellesley, MA, USA) LS50 spectrofluorimeter upon excitation at 294 nm.

### Characterization of aggregation states and oligomer heterogeneity

If not otherwise indicated, all experiments were carried out after at least 12 h of incubation of Hc against the desired buffer. Gel-filtration chromatography was carried out with a Pharmacia (Uppsala, Sweden) FPLC equipped with a Superose 6H 10/30 analytical column or with a HighLoad 26/60 Superdex 200 or a Fractogel XK 26/100 preparative grade column. Dodecameric, hexameric and monomeric Hc from *Car. aestuarii* [34] were used to calibrate the column. The columns were equilibrated with 50 mM Tris/HCl, pH 7.5, containing either 20 mM CaCl<sub>2</sub> or 10 mM EDTA to stabilize either the dodecameric or the monomeric structure, respectively.

Molecular mass determinations were carried out by light scattering analysis of the material eluted through a gel filtration column (Superose 6HR 10/30 analytical column; Pharmacia). The experiments were performed with a DAWN DSP photometer (Wyatt Technology, Santa Barbara, CA, USA;  $\lambda = 632.8\text{ nm}$ ) equipped with an HPLC HP 1100 pump (Hewlett Packard, Palo Alto, CA, USA). The molecular mass was calculated using the ASTRA software, employing the Rayleigh ratio:

$$R_0 = [2\pi^2 n_0^2 (dn/dc)^2 / A\lambda^4] \cdot M \cdot C = K \cdot M \cdot C$$

where  $n_0$  is the refraction index of the buffer (1.332),  $dn/dc$  the change of refraction index of the buffer owing to the presence of Hc (0.17 as a typical value for proteins),  $A$  is Avogadro's number,  $\lambda$  is the laser wavelength,  $M$  the molecular mass and  $C$  the protein concentration.

Dissociating conditions involved 50 mM Tris/HCl, 10 mM EDTA, pH > 8.5. The protein was dialyzed against the appropriate buffer at 4 °C for 12 h prior to chromatographic analysis.

Ion exchange chromatography was carried out with a MonoQ HR 5/5 using a 0–1.0 M NaCl gradient.

Native PAGE was carried out using a Mod. VP80 Electrofor vertical slab gel apparatus at pH 7.5. *Car. aestuarii* [34] or *E. californicum* Hc [56,57] were used as references. SDS/PAGE was carried out according to Fling & Gregerson [58].

Gel filtration experiments, using a Superose 6H 30/10 column, were carried out at different concentrations of NaSCN or NaClO<sub>4</sub>. Prior to chromatography, Hc ( $\approx 1\text{ mL}$ ) was dialysed against 100 mL of the desired buffer for 12 h.

### Oxygen-binding measurements

The oxygen binding to *P. monodon* Hc has been studied using two methods. The first is the tonometric method, as described in Molon *et al.* [19], and is based on the spectrophotometric determination of the intensity of the 340 nm absorption band caused by the peroxide-to-Cu(II) charge transfer transition. The second is the fluorimetric-polarographic method based on the difference in intrinsic tryptophan fluorescence quantum yield between deoxy- and oxy-Hc and on the direct determination of oxygen concentration by means of a Clark electrode [59,60]. With both approaches the fractional saturation of Hc ( $\theta$ ) was determined as described in Molon *et al.* [19].

### Sequence data and multiple alignment

The SwissProt and NCBI accession numbers for the complete amino acid sequences of 15 crustacean Hcs are presented in the legend to Table 1. For the analysis of Hc primary structures, the tools provided by the ExPASy Molecular Biology Server of the Swiss Institute of Bioinformatics (<http://www.expasy.ch>) were used. A multiple alignment was carried out with CLUSTALW, and the result was controlled considering the two conservative binding-site regions, according to Burmester [13]. From these alignments we were able to compare the amino acids in the positions involved in the interaction areas between monomers, which are responsible for the stability of hexameric form [9]. The amino acid positions are numbered following the sequence of *Panulirus* Hc subunit a throughout.

### Analysis of oxygen-binding curves

#### MWC model

The oxygen-binding curves of hexameric Hc from *P. monodon* were analysed according to the MWC model using the following binding polynomial:

$$P_{\text{MWC}} = (1 + K_r x)^n + I_0 (1 + K_t x)^n = P_r^n + I_0 P_t^n \quad (1)$$

Thus, the molecule can adopt two different conformations ( $t$  and  $r$ ) that are characterized by binding constants  $K_t$  and  $K_r$ . The size of the allosteric unit is  $n$ . The allosteric

equilibrium constant,  $l_o$ , describes the ratio of conformations r and t in the absence of ligand:

$$l_o = \frac{[t_o]}{[r_o]}$$

### Three-state MWC model

An extension of the simple two-state MWC model is a version where a third conformation available for the allosteric unit is introduced. This three-state MWC model is characterized by the following binding polynomial:

$$P_{3\text{-state}} = (1 + K_r x)^n + l_t (1 + K_t x)^n + l_s (1 + K_s x)^n = P_r^n + l_t P_t^n + l_s P_s^n \quad (2)$$

Here, the allosteric equilibrium constants again refer to the unligated states of the conformations available and are defined by:

$$l_t = \frac{[t_o]}{[r_o]} \quad l_s = \frac{[s_o]}{[r_o]}$$

### Nested MWC model

For analysis of the 12-meric Hc, the nested MWC model [30] was applied in the following form [61]:

$$P_{\text{nest}} = P_R^2 + \Lambda P_T^2 = (P_{rR}^6 + l_R P_{tR}^6)^2 + \Lambda (P_{rT}^6 + l_T P_{tT}^6)^2$$

$$\Lambda = L \frac{(1 + l_R)^2}{(1 + l_T)^2}$$

$$P_{\alpha\beta} = 1 + K_{\alpha\beta} x$$

$$\alpha\beta = rR, tR, rT, tT$$

In this model, a number of six subunits form an allosteric unit according to the MWC model, and can adopt two basic conformations (r and t). However, when these allosteric units again assemble to a larger structure, consisting of two copies of the hexameric allosteric units, additional constraints are imposed on the conformations. The  $2 \times 6$  structure can again be considered as a (large) allosteric unit, which can adopt two conformations (R and T). When the  $2 \times 6$ -mer is in the R-state, the nested 6-meric allosteric units can adopt the two conformations rR and tR. When the  $2 \times 6$ -mer is in the T-state, two other conformations (rT and tT) are available. Thus, the conformation of the  $2 \times 6$ -mer defines the conformation of the nested 6-mers in a hierarchical manner. The equilibrium between unliganded  $R_o$  and  $T_o$  states is given by  $L = [T_o]/[R_o]$ . The allosteric equilibrium constants,  $l_R$  and  $l_T$ , correspond to  $l_R = [tR_o]/[rR_o]$  and  $l_T = [tT_o]/[rT_o]$ . The allosteric equilibrium constants optimized in the analysis were  $l_R$ ,  $l_T$  and  $\Lambda$ . The value for  $L$  can then be calculated based on Eqn (3).

The oxygen-saturation curve  $\Theta$  is obtained from the binding polynomial as

$$\Theta = \frac{\partial \ln P}{n \partial \ln x} \quad (3)$$

where  $x$  is the oxygen partial pressure and  $n$  the size of the largest allosteric unit.

For each of the possible models, the resulting equations for the degree of saturation  $\Theta$  in dependence on the oxygen partial pressure were fitted to the data. In order to allow for slight deviations in the initial ( $f_o$ ) and final ( $f$ ) amplitude, the binding data were analyzed employing the following equation:

$$\theta_{\text{observed}} = (f - f_o)\theta + f_o. \quad (4)$$

The fitting routine was based on a nonlinear regression analysis (Levenberg–Marquardt routine) incorporated into the program SIGMA PLOT (SPSS, Chicago, IL, USA).

### Acknowledgements

This work was supported by grants De 414/8-1,2; SFB 625 B5; MURST.

### References

- Ellerton HD, Ellerton NF & Robinson HA (1983) Hemocyanin – a current perspective. *Prog Biophys Mol Biol* **41**, 143–248.
- Mangum CP, Scott JL, Black RE, Miller KI & Van Holde KE (1985) Centipede hemocyanin: its structure and its implications for arthropod phylogeny. *Proc Natl Acad Sci USA* **82**, 3721–3725.
- Markl J & Decker H (1992) Molecular structure of arthropod hemocyanins. *Adv Comp Environ Physiol* **13**, 325–376.
- Kusche K, Ruhberg H & Burmester T (2002) A hemocyanin from the Onychophora and the emergence of respiratory proteins. *Proc Natl Acad Sci USA* **99**, 10545–10548.
- Hagner-Holler S, Schoen A, Erker W, Marden JH, Rupprecht R, Decker H & Burmester T (2004) A respiratory hemocyanin from an insect. *Proc Natl Acad Sci USA* **101**, 871–874.
- Sanchez D, Ganfornina MD, Gutierrez G & Bastiani MJ (1998) Molecular characterization and phylogenetic relationships of a protein with potential oxygen-binding capabilities in the grasshopper embryo. A hemocyanin in insects? *Mol Biol Evol* **15**, 415–426.
- Linzen B, Soeter NM, Riggs AF, Schneider HJ, Schartau W, Moore MD, Yokota E, Behrens PQ, Nakashima H, Takagi T *et al.* (1985) The structure of arthropod hemocyanins. *Science* **229**, 519–524.
- Hazes B, Magnus KA, Bonaventura C, Bonaventura J, Dauter Z, Kalk KH & Hol WG (1993) Crystal structure

- of deoxygenated *Limulus polyphemus* subunit II hemocyanin at 2.18 Å resolution: clues for a mechanism for allosteric regulation. *Protein Sci* **2**, 597–619.
- 9 Volbeda A & Hol WG (1989) Crystal structure of hexameric haemocyanin from *Panulirus interruptus* refined at 3.2 Å resolution. *J Mol Biol* **209**, 249–379.
  - 10 Bijlholt MM, van Heel MG & van Bruggen EF (1982) Comparison of 4 x 6-meric hemocyanins from three different arthropods using computer alignment and correspondence analysis. *J Mol Biol* **161**, 139–153.
  - 11 de Haas F & van Bruggen EF (1994) The interhexameric contacts in the four-hexameric hemocyanin from the tarantula *Eurypelma californicum*. A tentative mechanism for cooperative behavior. *J Mol Biol* **237**, 464–478.
  - 12 Meissner U, Stohr M, Kusche K, Burmester T, Stark H, Harris JR, Orlova EV & Markl J (2003) Quaternary structure of the European spiny lobster (*Palinurus elephas*) 1x6-mer hemocyanin from cryoEM and amino acid sequence data. *J Mol Biol* **325**, 99–109.
  - 13 Burmester T (2001) Molecular evolution of the arthropod hemocyanin superfamily. *Mol Biol Evol* **18**, 184–195.
  - 14 Magnus KA, Hazes B, Ton-That H, Bonaventura C, Bonaventura J & Hol WG (1994) Crystallographic analysis of oxygenated and deoxygenated states of arthropod hemocyanin shows unusual differences. *Proteins* **19**, 302–309.
  - 15 Voit R, Feldmaier-Fuchs G, Schweikardt T, Decker H & Burmester T (2000) Complete sequence of the 24-mer hemocyanin of the tarantula *Eurypelma californicum*. Structure and intramolecular evolution of the subunits. *J Biol Chem* **275**, 39339–39344.
  - 16 Sullivan B, Bonaventura J & Bonaventura C (1974) Functional differences in the multiple hemocyanins of the horseshoe crab, *Limulus polyphemus* L. *Proc Natl Acad Sci USA* **71**, 2558–2562.
  - 17 Lamy J, Bijlholt MC, Sizaret PY & van Bruggen EF (1981) Quaternary structure of scorpion (*Androctonus australis*) hemocyanin. Localization of subunits with immunological methods and electron microscopy. *Biochemistry* **20**, 1849–1856.
  - 18 Decker H, Savel-Niemann A, Korschenhausen D, Eckerskorn E & Markl J (1989) Allosteric oxygen-binding properties of reassembled tarantula (*Eurypelma californicum*) hemocyanin with incorporated apo- or met-subunits. *Biol Chem Hoppe Seyler* **370**, 511–523.
  - 19 Molon A, Di Muro P, Bubacco L, Vasilyev V, Salvato B, Beltramini M, Conze W, Hellmann N & Decker H (2000) Molecular heterogeneity of the hemocyanin isolated from the king crab *Paralithodes camtschaticae*. *Eur J Biochem* **267**, 7046–7057.
  - 20 Bellelli A, Giardina B, Corda M, Pellegrini MG, Cau A, Condo SG & Brunori M (1988) Sexual and seasonal variability of lobster hemocyanin. *Comp Biochem Physiol* **91A**, 445–449.
  - 21 Mangum CP, Greaves J & Rainer JS (1991) Oligomer composition and oxygen binding of the hemocyanin of the blue crab *Callinectes sapidus*. *Biol Bull* **181**, 453–458.
  - 22 Mangum CP (1994) Subunit composition of hemocyanins of *Callinectes sapidus*: phenotypes from naturally hypoxic waters and isolated oligomers. *Comp Biochem Physiol Biochem Mol Biol* **108**, 537–541.
  - 23 Terwilliger NB (1998) Functional adaptations of oxygen-transport proteins. *J Exp Biol* **201**, 1085–1098.
  - 24 Kitajima N, Fujisawa K, Fujimoto C, Moro-oka Y, Hashimoto S, Kitagawa T, Toriumi K, Tatsumi K & Nakamura A (1992) A new model for dioxygen binding in hemocyanin. Synthesis, characterization and molecular structure of the  $\mu$ - $\eta^2$ : $\eta^2$  peroxo dinuclear copper(II) complexes, [Cu (HB(3,5-R<sub>2</sub>pz)<sub>3</sub>)<sub>2</sub>(O<sub>2</sub>) (R=*i*-Pr and Ph). *J Am Chem Soc* **114**, 1277–1291.
  - 25 Solomon EI (1981) Binuclear copper active site. In: *Copper Proteins* (Spiro TG, ed.), pp. 41–108. Academic Press, New York.
  - 26 Connelly PR, Johnson CR, Robert CH, Bak HJ & Gill SJ (1989) Binding of oxygen and carbon monoxide to the hemocyanin from the spiny lobster. *J Mol Biol* **207**, 829–832.
  - 27 Savel-Niemann A, Markl J & Linzen B (1988) Hemocyanins in spiders. XXII. Range of allosteric interaction in a four-hexamer hemocyanin. Co-operativity and Bohr effect in dissociation intermediates. *J Mol Biol* **204**, 385–395.
  - 28 Decker H, Robert CH & Gill SJ (1986) Nesting – an extension of the allosteric model and its application to tarantula hemocyanin. In: *Invertebrate Oxygen Carriers* (Linzen B, ed.), pp. 383–388. Springer, Heidelberg.
  - 29 Robert CH, Decker H, Richey B, Gill SJ & Wyman J (1987) Nesting: hierarchies of allosteric interactions. *Proc Natl Acad Sci USA* **84**, 1891–1895.
  - 30 Decker H & Sterner R (1990) Nested allostery of arthropodan hemocyanin (*Eurypelma californicum* and *Homarus americanus*). The role of protons. *J Mol Biol* **211**, 281–293.
  - 31 Hartmann H & Decker H (2002) All hierarchical levels are involved in conformational transitions of the 4, x 6-meric tarantula hemocyanin upon oxygenation. *Biochim Biophys Acta* **1601**, 132–137.
  - 32 Hartmann H & Decker H (2004) Small-angle scattering techniques for analyzing conformational transitions in hemocyanins. *Methods Enzymol* **379**, 81–106.
  - 33 Hartmann H, Lohkamp B, Hellmann N & Decker H (2001) The allosteric effector 1-lactate induces a conformational change of 2x6-meric lobster hemocyanin in the oxy state as revealed by small angle x-ray scattering. *J Biol Chem* **276**, 19954–19958.
  - 34 Dainese E, Di Muro P, Beltramini M, Salvato B & Decker H (1998) Subunits composition and allosteric control in *Carcinus aestuarii* hemocyanin. *Eur J Biochem* **256**, 350–358.

- 35 Schram FR (2001) Phylogeny of decapods: moving towards a consensus. *Hydrobiologia* **449**, 1–20.
- 36 Mason PE, Neilson GW, Dempsey CE, Barnes AC & Cruickshank JM (2003) The hydration structure of guanidinium and thiocyanate ions: implications for protein stability in aqueous solution. *Proc Natl Acad Sci USA* **100**, 4557–4561.
- 37 Shortle D, Meeker AK & Gerring SL (1989) Effects of denaturants at low concentrations on the reversible denaturation of staphylococcal nuclease. *Arch Biochem Biophys* **272**, 103–113.
- 38 Scholtz JM & Baldwin RL (1993) Perchlorate-induced denaturation of ribonuclease A: investigation of possible folding intermediates. *Biochemistry* **32**, 4604–4608.
- 39 Maity H, Eftink M & R (2004) Perchlorate-induced conformational transition of Staphylococcal nuclease: evidence for an equilibrium unfolding intermediate. *Arch Biochem Biophys* **431**, 119–123.
- 40 Sellos D, Lemoine S & Van Wormhoudt A (1997) Molecular cloning of hemocyanin cDNA from *Penaeus vannamei* (Crustacea, Decapoda): structure, evolution and physiological aspects. *FEBS Lett* **407**, 153–158.
- 41 Mangum CP & Weiland AL (1975) The function of hemocyanin in respiration of the blue crab *Callinectes sapidus*. *J Exp Zool* **193**, 257–264.
- 42 Decker H & Foll R (2000) Temperature adaptation influences the aggregation state of hemocyanin from *Astacus leptodactylus*. *Comp Biochem Physiol A: Mol Integr Physiol* **127**, 147–154.
- 43 Brouwer M, Bonaventura C & Bonaventura J (1978) Analysis of the effect of three different allosteric ligands on oxygen binding by hemocyanin of the shrimp, *Penaeus setiferus*. *Biochemistry* **17**, 2148–2154.
- 44 Favilla R, Goldoni M, Mazzini A, Di Muro P, Salvato B & Beltramini M (2002) Guanidinium chloride induced unfolding of a hemocyanin subunit from *Carcinus aestuarii*. I. Apo form. *Biochem Biophys Acta* **1597**, 42–50.
- 45 Favilla R, Goldoni M, Del Signore F, Di Muro P, Salvato B & Beltramini M (2002) Guanidinium chloride induced unfolding of a hemocyanin subunit from *Carcinus aestuarii*. II. Holo form. *Biochem Biophys Acta* **1597**, 51–59.
- 46 Makino N (1989) Hemocyanin from *Tachypleus gigas*. II. Cooperative interactions of the subunits. *J Biochem (Tokyo)* **106**, 423–429.
- 47 Richey B, Decker H & Gill SJ (1985) Binding of oxygen and carbon monoxide to arthropod hemocyanin: an allosteric analysis. *Biochemistry* **24**, 109–117.
- 48 Johnson BA, Bonaventura C & Bonaventura J (1988) Allostery in *Callinectes sapidus* hemocyanin: cooperative oxygen binding and interactions with L-lactate, calcium, and protons. *Biochemistry* **27**, 1995–2001.
- 49 van Holde KE & Miller KI (1995) Hemocyanins. *Adv Protein Chem* **47**, 1–81.
- 50 Truchot JP (1980) Lactate increases the oxygen affinity of crab hemocyanin. *J Exp Zool* **214**, 205–208.
- 51 Lallier F & Truchot JP (1989) Hemolymph oxygen transport during environmental hypoxia in the shore crab, *Carcinus maenas*. *Respir Physiol* **77**, 323–336.
- 52 Chausson F, Bridges CR, Sarradin PM, Green BN, Riso R, Caprais JC & Lallier FH (2001) Structural and functional properties of hemocyanin from *Cyanagraea praedator*, a deep-sea hydrothermal vent crab. *Proteins* **45**, 351–359.
- 53 Truchot JP (1992) Respiratory function of arthropod hemocyanins. *Comp Environ Physiol* **13**, 377–410.
- 54 Bubacco L, Magliozzo RS, Beltramini M, Salvato B & Peisach J (1992) Preparation and spectroscopic characterization of a coupled binuclear center in cobalt(II)-substituted hemocyanin. *Biochemistry* **31**, 9294–9303.
- 55 Klotz IM & Klotz TA (1955) Oxygen-carrying proteins: a comparison of the oxygenation reaction in hemocyanin and hemerythrin with that in hemoglobin. *Science* **121**, 477–480.
- 56 Markl J, Hofer A, Bauer G, Markl A, Kempter B, Brenzinger M & Linzen B (1979) Subunit heterogeneity in arthropod hemocyanins. II. Crustacea. *J Comp Physiol* **133**, 167–175.
- 57 Markl J, Strych W, Schartau W, Schneider HJ, Schoberl P & Linzen B (1979) Hemocyanins in spiders, VI [1]. Comparison of the polypeptide chains of *Eurypelma californicum* hemocyanin. *Hoppe Seylers Z Physiol Chem* **360**, 639–650.
- 58 Fling SP & Gregerson DS (1986) Peptide and protein molecular weight determination by electrophoresis using a high-molarity tris buffer system without urea. *Anal Biochem* **155**, 83–88.
- 59 Loewe R (1978) Hemocyanins in spiders. V. Fluorimetric recording of oxygen binding curves, and its application to the analysis of allosteric interactions in *Eurypelma californicum* hemocyanin. *J Comp Physiol* **128**, 161–168.
- 60 Decker H, Markl J, Loewe R & Linzen B (1979) Hemocyanins in spiders, VIII. Oxygen affinity of the individual subunits isolated from *Eurypelma californicum* hemocyanin. *Hoppe Seylers Z Physiol Chem* **360**, 1505–1507.
- 61 Hellmann N (2004) Bohr-effect and buffering capacity of hemocyanin from the tarantula *E. californicum*. *Biophys Chem* **109**, 157–167.